Spectrum of second-harmonic radiation generated from incoherent light

A. Stabinis, V. Pyragaite,* G. Tamošauskas, and A. Piskarskas
Department of Quantum Electronics, Vilnius University, Sauletekio Avenue 9, Building 3, LT-10222 Vilnius, Lithuania
(Received 15 April 2011; published 5 October 2011)

We report on the development of the theory of second-harmonic generation by an incoherent pump with broad angular and frequency spectra. We show that spatial as well as temporal walk-off effects in a nonlinear crystal result in angular dispersion of the second-harmonic radiation. We demonstrate that the acceptance angle in second-harmonic generation by incoherent light is caused by the width of the pump angular spectrum and the resulting angular dispersion of second-harmonic radiation but does not depend on crystal length. In this case the frequency spectrum of second-harmonic radiation is determined by its angular dispersion and the pump angular spectrum. The theory is supported by an experiment in which a $LiIO_3$ crystal was pumped by a tungsten halogen lamp.

DOI: 10.1103/PhysRevA.84.043813 PACS number(s): 42.25.Kb, 42.65.Ky

I. INTRODUCTION

Since its first demonstration in 1961 [1], second-harmonic (SH) generation has traditionally been studied in the framework of laser physics. Several papers published in the same decade [2–4] on the upconversion of incoherent light did not give rise to an extensive study of the subject. Meanwhile, laser-excited SH generation is frequently used for transformation of the frequency of laser radiation and it has already become a standard procedure. The main reason that research into incoherent pumping and its applications did not continue may be its low conversion efficiency, of the order of 10^{-12}. Nevertheless, the idea of incoherent excitation resulted in several interesting theoretical works. For example, in 2001 Picozzi and Haelterman showed that it is possible to generate a parametrically coherent signal by use of an incoherent pump [5,6]. Another wave, the idler, remains incoherent and the process takes place if the group velocities of the two incoherent waves, pump and idler, coincide and differ from the group velocity of the signal wave. Recently, in Ref. [7], it was shown that a similar effect can be observed in the process of SH generation from temporally incoherent light. It was shown that the SH frequency spectrum narrows and the conversion is more efficient if the proper angular dispersion of the fundamental wave is chosen. The predictions of Picozzi and Haelterman as well as of Piskarskas *et al*. [7] have not yet been confirmed experimentally. On the other hand, in the early experimental papers [2–4], an attempt was made to explain the observed phenomena, e.g., the conversion efficiency as well as SH spectral profiles were calculated and compared to the measured ones. Still a detailed theoretical overview of the problem is missing; for example, what determines the spectral width of the second harmonic?

So, in the present study we turn to a more realistic model than that in Refs. [5–7], which describes the fundamental wave as a spatially and temporally incoherent wave. It is revealed that both spatial and temporal walk-off have to be taken into account in order to explain the observed angular distribution of SH frequency components. It is demonstrated by the use of the phase-matching conditions as well as numerical calculations that the spectrum of the SH obeys an angular dispersion. The dispersion angle is determined by both spatial and temporal walk-off parameters. The result is confirmed experimentally. Further study shows that in the chosen nonlinear crystal ($LiIO_3$) the frequency bandwidth of the SH is determined by the angular bandwidth of the fundamental wave rather than by its frequency bandwidth. We demonstrate that SH generation can be effective even when the angular bandwidth of the pump exceeds by 100 times the acceptance angle of the nonlinear crystal. We present a theoretical formula which describes how the conversion efficiency of the SH is determined by the angular and frequency bandwidths of the fundamental wave. It is interesting to note that a similar expression was obtained in Ref. [8], where SH generation from a regular wave in the presence of both temporal and spatial walk-off was investigated. Finally, it is demonstrated that SH spectral radiance grows faster than linearly with the crystal length, and there exists the possibility of exceeding the spectral radiance of the fundamental wave by SH generation from an incoherent source.

The paper is organized as follows. The theory is derived in Sec. II starting with analysis of the angular dispersion law of the SH determined by the phase-matching conditions. The numerically calculated spectra are presented and discussed in Sec. III. In Sec. IV the experimental results obtained with a tungsten halogen lamp pump are compared to the ones calculated theoretically. The conclusions are drawn in Sec. V.

II. PHASE-MATCHING CONDITIONS

Let us examine for simplicity the phase-matching conditions of the SH generation process in the xz plane:

$$k_1 \sin\theta_1 + k_2 \sin\theta_2 = k_3 \sin\theta_3, \tag{1a}$$

$$k_1 \cos\theta_1 + k_2 \cos\theta_2 = k_3 \cos\theta_3, \tag{1b}$$

$$\omega_1 + \omega_2 = \omega_3, \tag{1c}$$

where the indices 1, 2, and 3 correspond to the first and second fundamental waves and the SH wave, respectively. k is the wave number and ω the cyclic frequency. The angle θ is the angle in the xz plane with respect to the z axis. The type-I phase matching in a nonlinear crystal is considered, so $k_1 = k_1(\omega_1)$, $k_2 = k_2(\omega_2)$, and $k_3 = k_3(\omega_3,\theta_3)$. The z axis corresponds to the

*viktorija.pyragaite@ff.vu.lt

direction of collinear phase matching at the same frequency ω_{10} of both fundamental waves:

$$k_1(\omega_{10}) = k_2(\omega_{10}) = k_3(2\omega_{10},0)/2. \tag{2}$$

Let us denote $k_{10} = k_1(\omega_{10})$, $k_{30} = k_3(\omega_{30},0)$, and $\omega_{30} = 2\omega_{10}$. Further, we bring into consideration the frequency shifts Ω_j:

$$\omega_j = \omega_{j0} + \Omega_j, \quad j = 1,2,3. \tag{3}$$

In the experiment discussed below these shifts satisfy the condition $\Omega_j/\omega_{j0} < 0.3$. Then we can use the Taylor expansion of k_j: $k_1 = k_{10} + \Omega_1/u_{10} + g_{10}\Omega_1^2/2$, $k_2 = k_{20} + \Omega_2/u_{20} + g_{20}\Omega_2^2/2$, $k_3 = k_{30} + \Omega_3/u_{30} + g_{30}\Omega_3^2/2 + k_{30}\gamma\theta_3$, where u_{j0} is the group velocity, $u_{j0}^{-1} = (dk_j/d\omega_j)_{\omega_{j0}}$, and $g_{j0} = (d^2k_j/d\omega_j^2)_{\omega_{j0}}$ is the group velocity dispersion coefficient. $\gamma < 0$ is the walk-off angle in a $LiIO_3$ crystal. From Eqs. (1c) and (3) it follows that

$$\Omega_1 + \Omega_2 = \Omega_3. \tag{4}$$

Let us consider the paraxial approximation. Then $\sin\theta \approx \theta$, $\cos\theta \approx 1 - \theta^2/2$, and from Eqs. (1a) and (2) we obtain

$$\theta_1 + \theta_2 \approx 2\theta_3. \tag{5}$$

By use of Eqs. (1), (4), and (5) we find the angular dispersion relation of the fundamental wave at exact phase matching:

$$m_0^2\left(\frac{\Omega_1}{\omega_{10}} - D\right)^2 - (\theta_1 - \theta_3)^2 - 2h(D,\theta_3) = 0, \tag{6}$$

where

$$h(D,\theta_3) = \frac{\nu c D}{n_{10}} + m_0^2\left(\frac{g_{30}}{g_{10}} - \frac{1}{2}\right)D^2 - |\gamma|\theta_3, \tag{7}$$

$m_0^2 = \omega_{10}^2 g_{10}/k_{10}$, $D = \Omega_3/\omega_{30}$, $\nu = 1/u_{30} - 1/u_{10}$ is the group velocity mismatch, and n_{10} is the refractive index of the fundamental wave at frequency ω_{10}. As a result, the SH wave at fixed values Ω_3 and θ_3 is generated in a phase-matched way by various fundamental plane waves whose frequencies Ω_1 and angles θ_1 obey the dispersion relation (hyperbola) given by Eq. (6). The corresponding dispersion curves of the fundamental wave are presented in Fig. 1. These and further calculations were performed for type-I phase matching in a $LiIO_3$ crystal. The Sellmeier equations from Ref. [9] were adopted. The points lying on the dashed line ($h = 0$) correspond to the collinear phase matching of fundamental waves at equal frequencies $\Omega_1 = \Omega_2 = \Omega_3/2$. In this case the corresponding angular dispersion law of the SH wave is

$$\frac{\nu c D_0}{n_{10}} + m_0^2\left(\frac{g_{30}}{g_{10}} - \frac{1}{2}\right)D_0^2 - |\gamma|\theta_{30} = 0. \tag{8}$$

If we neglect the small D_0^2 values, then $h = 0$ yields a linear angular dispersion law for the spectrum of the SH wave at collinear interaction:

$$D_0 \approx \frac{|\gamma| n_{10}}{\nu c}\theta_{30}. \tag{9}$$

The dispersion is determined by the walk-off angle γ as well as the temporal walk-off ν. In this case the angular dispersion curves of the fundamental wave are two intersecting straight lines. If $D \neq D_0$ and $\theta_3 \neq \theta_{30}$, then $h \neq 0$, and the angular dispersion curve of the fundamental wave is a hyperbola (Fig. 1).

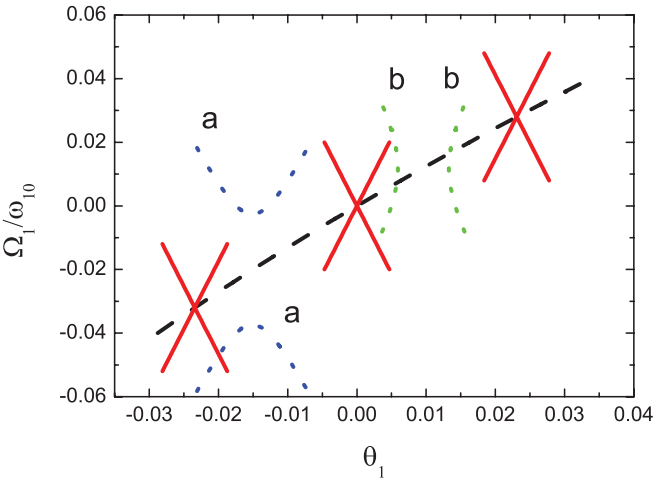

FIG. 1. (Color online) The angular dispersion curves of the fundamental wave at exact phase matching for $h = 0$ (intersecting straight solid red lines) and $h \neq 0$ (hyperbolas). $h < 0$, $D - D_0 = 1.4 \times 10^{-4}$, $\theta_3 - \theta_{30} = 10^{-4}$ rad (a, dotted blue curves); $h > 0$, $D - D_0 = -10^{-4}$, $\theta_3 - \theta_{30} = 0.8 \times 10^{-4}$ rad (b, dotted green curves). The collinear phase matching of fundamental waves at equal frequencies is also shown ($\Omega_1 = \Omega_2 = \Omega_3/2$, $h = 0$, dashed black line). $LiIO_3$ crystal with central fundamental wavelength $\lambda_{10} = 905$ nm. θ_1 is given in radians.

III. COUPLED EQUATIONS OF SECOND-HARMONIC GENERATION

Now let us examine the coupled equations of SH generation which describe the variation of the complex amplitudes A_j in a nonlinear medium in the presence of temporal as well as spatial walk-off:

$$\frac{\partial A_1}{\partial z} = i\frac{g_{10}}{2}\frac{\partial^2 A_1}{\partial t^2} - \frac{i}{2k_{10}}\frac{\partial^2 A_1}{\partial x^2} + \sigma A_1^* A_3, \tag{10a}$$

$$\frac{\partial A_3}{\partial z} = -\nu\frac{\partial A_3}{\partial t} + \gamma\frac{\partial A_3}{\partial x} + i\frac{g_{30}}{2}\frac{\partial^2 A_3}{\partial t^2} - \frac{i}{2k_{30}}\frac{\partial^2 A_3}{\partial x^2} + \sigma A_1^2; \tag{10b}$$

here $\sigma = d_{\rm ef}\omega_{30}^2/(2c^2k_{30})$ is the coupling coefficient, and $d_{\rm ef}$ is the effective quadratic susceptibility. For simplicity only one transverse coordinate x is taken into account; z is the longitudinal coordinate, and t is the time.

We note that Eqs. (10) coincide with Eqs. (31) in Ref. [7] when $\gamma = 0$. In Ref. [7] it was supposed that the interacting waves are of high spatial coherence. Now we assume that the fundamental wave is spatially incoherent, so the spatial walk-off has to be taken into account, $\gamma \neq 0$.

Let us bring into the consideration the spectral radiance $S_j = \frac{1}{4\pi^2}\langle|a_j|^2\rangle$, where a_j is the Fourier transform of A_j:

$$a_j(\Omega,\beta) = \int_{-\infty}^{\infty}\int_{-\infty}^{\infty} A_j(t,x)\exp[-i(\Omega t - \beta x)]dt\,dx. \tag{11}$$

The angular brackets $\langle\cdots\rangle$ denote the average over the realizations. We assume that the amplitude of the fundamental

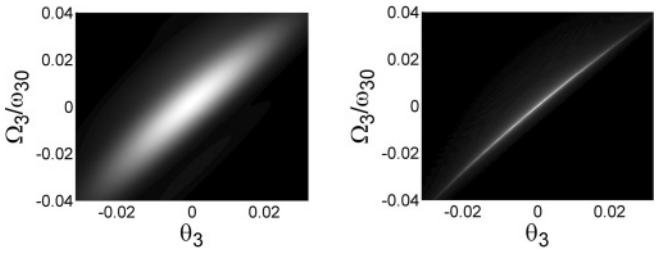

FIG. 2. Angular distribution of SH frequency components $S_3(D,\theta_3)$, calculated by the use of Eq. (13). Crystal length z 200 μm (left) and 2 cm (right). $LiIO_3$ crystal, type-I phase matching. Central wavelength of the fundamental wave $\lambda_{10} = 905$ nm. Parameters $a = 0.28$, $b = 0.032$. θ_3 is given in radians.

wave $A_1(t,x)$ is a stationary Gaussian noise and the spectral radiance S_1 is Gaussian:

$$S_1 = S_0 \exp\left[-\frac{\Omega_1^2}{\Delta\Omega_1^2} - \frac{\theta_1^2}{\Delta\theta_1^2}\right], \tag{12}$$

where $\Delta\Omega_1$ and $\Delta\theta_1$ are the bandwidths of the frequency and angular spectra, respectively. Then, if the nonlinear term in Eq. (10a) is neglected, the spectral radiance of the SH radiation reads [7]

$$\frac{S_3(D,\theta_3,z)}{S_0} = \frac{2}{\pi ab}\left(\frac{z}{L_n}\right)^2 \exp\left[-2\frac{D^2}{a^2} - 2\frac{\theta_3^2}{b^2}\right] \times \int_{-\infty}^{\infty}\int_{-\infty}^{\infty} \frac{\sin^2 F}{F^2} \exp\left[-2\frac{\xi^2}{a^2} - 2\frac{\eta^2}{b^2}\right] d\xi\, d\eta, \tag{13}$$

where $F = \alpha[m_0^2\xi^2 - \eta^2 - 2h]$, $\alpha = \frac{\pi z n_{10}}{\lambda_{10}}$, h is defined by Eq. (7), $a = \Delta\Omega_1/\omega_{10}$, $b \equiv \Delta\theta_1$, and λ_{10} is the central wavelength of the fundamental wave. $L_n = (\sigma A_{10})^{-1}$ is the nonlinear interaction length, where $A_{10} = \langle|A_1|^2\rangle^{1/2}$ is the average amplitude of the fundamental wave at $z = 0$. An analysis of Eq. (13) shows that, when $\alpha \gg 1$ or $z \gg \lambda_{10}$, a narrow maximum of the spectrum S_3 for fixed value θ_3 is obtained at $h = 0$. The condition $h = 0$ corresponds to the collinear phase matching (dashed line in Fig. 1) discussed in the previous section. The calculated angular distributions of SH frequency components at two different crystal lengths are presented in Fig. 2. Both spectra clearly show the presence of angular dispersion. We note that the width $\Delta\theta_3$ of the SH angular spectrum depends on the parameter b, but does not depend on crystal length (compare Figs. 2 left and right) as it should in the case of monochromatic fundamental radiation. So the acceptance angle in SH generation by incoherent waves due to angular dispersion of the SH wave is caused by the width of the angular spectrum of the fundamental wave $\Delta\theta_1$. In this case the width $\Delta\Omega_3$ of the SH frequency spectrum is determined by the parameter b (or $\Delta\theta_1$) as well as by the angular dispersion of SH radiation. The calculated dependences of the SH central spectral component $S_{30} = S_3(0,0)$ and the frequency bandwidth $\Delta\Omega_3^n$ at $\theta_3 = 0$ (normalized to its initial value at $z \approx 0$) on the propagation length in a nonlinear crystal are presented in Fig. 3. So a significant monochromatization of SH radiation (by three orders of magnitude) at a fixed value θ_3 takes place in a 2-cm-length crystal. By use of Eq. (13) we find that $S_{30} \sim z^2$ as $z \to 0$ and $S_{30} \sim z^{3/2}$ at $z \geqslant 1$ mm and $b \ll a$. So the SH spectral radiance can exceed the spectral radiance of the fundamental wave [Fig. 3 (solid line)]. In this case the nonlinear term in Eq. (10a) could be omitted because the conversion efficiency at $z = 40$ cm is equal to 0.44. The conversion efficiency was calculated by the use of Eq. (18) given below. In practical applications, extension of the effective length of the crystal may be achieved by locking the SH radiation into the cavity.

Further we will calculate the intensity of the SH wave, $I_3 \sim \langle|A_3|^2\rangle$, where

$$\langle|A_3|^2\rangle = \frac{1}{4\pi^2}\int_{-\infty}^{\infty}\int_{-\infty}^{\infty} S_3(\Omega_3,\beta_3)\, d\Omega_3\, d\beta_3. \tag{14}$$

By use of the approximations $\sin^2 F/F^2 \approx \exp(-\kappa^2 F^2)$, $\kappa \approx \frac{1}{\sqrt{3}} \approx 0.58$, and in the case of linear angular dispersion of the SH wave ($h \approx \frac{\nu c D}{n_{10}} - |\gamma|\theta_3$), integration of the spectrum S_3 over Ω_3 and β_3 gives

$$\langle|A_3|^2\rangle = \frac{4\omega_{10}k_{10}z^2 S_0}{m_0\kappa\alpha L_n^2}\int_0^{\infty}\int_0^{\pi} e^{-\rho^2\cos^2\varphi - p\rho - q\rho\cos\varphi}\, d\rho\, d\varphi, \tag{15}$$

where

$$p = \sqrt{1 + 2\kappa^2\alpha^2\left[\left(\frac{\nu c}{n_{10}}a\right)^2 + \gamma^2 b^2\right]}\left(\frac{1}{m_0^2 a^2} + \frac{1}{b^2}\right)\Big/(\kappa\alpha),$$
$$q = \sqrt{1 + 2\kappa^2\alpha^2\left[\left(\frac{\nu c}{n_{10}}a\right)^2 + \gamma^2 b^2\right]}\left(\frac{1}{m_0^2 a^2} - \frac{1}{b^2}\right)\Big/(\kappa\alpha). \tag{16}$$

In a 2-cm-long $LiIO_3$ crystal at $\lambda_{10} = 905$ nm as in experiment we find $\kappa\alpha \approx 8 \times 10^4$. If

$$p + q \gg 1 \quad \text{and} \quad p - q \gg 1, \tag{17}$$

then the term $\rho^2\cos^2\varphi$ in the power of the exponent of Eq. (15) can be neglected, and $\int_0^{\infty}\int_0^{\pi}\exp(-p\rho - q\rho\cos\varphi)d\rho\, d\varphi = \pi(p^2 - q^2)^{-1/2}$. In this case, taking into account that $L_n^{-2} = \frac{1}{4\pi}\sigma^2 S_0\omega_{10}k_{10}ab$, Eq. (15) at large values $\kappa\alpha \gg 1$ gives

$$\langle|A_3|^2\rangle = \frac{4\sqrt{2}\pi^{5/2}n_{10}c^2\sigma^2 S_0^2}{\kappa\lambda_{10}^3}\frac{a^2b^2z}{\sqrt{(\nu ca/n_{10})^2 + \gamma^2 b^2}}; \tag{18}$$

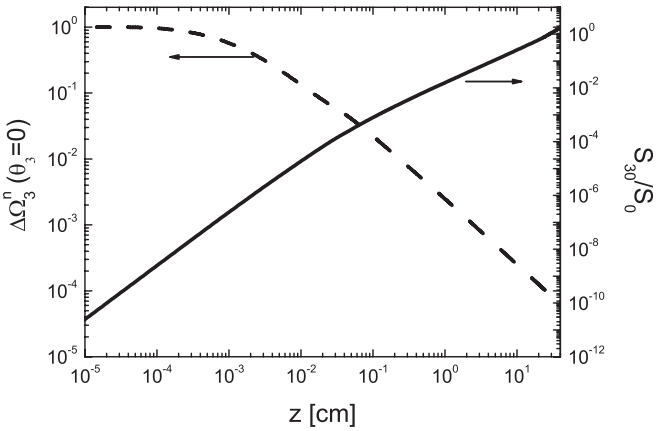

FIG. 3. Calculated S_{30}/S_0 (solid line) and normalized frequency bandwidth $\Delta\Omega_3^n$ of the SH at $\theta_3 = 0$ (dashed line). $LiIO_3$ crystal, type-I phase matching. Central wavelength of the fundamental wave $\lambda_{10} = 905$ nm. Parameters $a = 0.28$, $b = 0.032$. Nonlinear interaction length $L_n = 2$ cm.

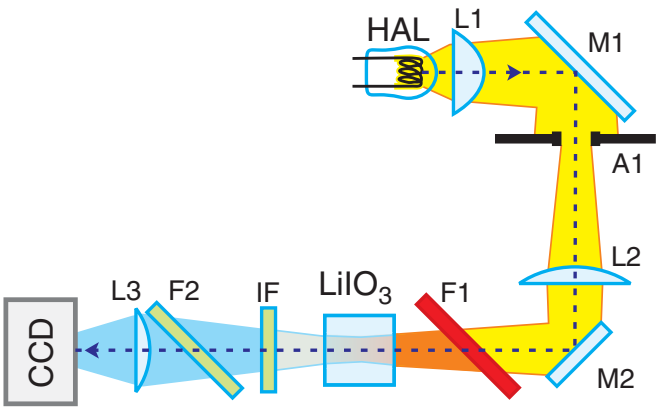

FIG. 4. (Color online) Simplified experimental setup: HAL, light source halogen lamp; $LiIO_3$, second-harmonic-generation crystal; CCD, light power sensor based on a CCD camera; F1, short-wave cutoff filter; IF, interference filter; F2, long-wave cutoff filter; L1,L2,L3, lenses; A1, aperture of spatial filter; M1, broadband dielectric mirror; M2, Au metallic mirror.

compare to Eq. (20) in Ref. [8]. For $a \gg b$ as in experiment the conditions (17) can be rewritten as $a \ll \frac{2\sqrt{2}\nu c}{n_{10}m_0^2} \approx 3.3, b^2 \ll \frac{2\sqrt{2}\nu c}{n_{10}} a \approx 0.18a$, and Eq. (18) takes the form

$$\langle |A_3|^2 \rangle \sim \sigma^2 S_0^2 z a b^2. \tag{19}$$

So the SH intensity in the one-dimensional (x) case depends quadratically on the width of the angular spectrum of the fundamental wave. This result is determined by the dispersion curves of the fundamental wave which are presented in Fig. 1. Each plane monochromatic SH wave is created in a phase-matched way by various fundamental waves whose frequencies Ω_1 and angles θ_1 obey the dispersion relation given by Eq. (6). For example, at $h = 0$ this dispersion curve is a straight line and its length is determined by the parameter b. Then the summation over all angles θ_1 leads to quadratic dependence of the SH intensity on the parameter b. We note that in the two-dimensional case (x,y) Eq. (19) can be written as

$$\langle |A_3|^2 \rangle \sim \sigma^2 S_0^2 z a b^4, \tag{20}$$

and for the SH power P_3 we obtain

$$P_3 \sim P_1^2 z/a, \tag{21}$$

where $P_1 \sim S_0 a b^2$ is the power of the fundamental wave. It means that the SH power rises by a second-order dependence on the pump power independently of its spatial content.

IV. EXPERIMENT

A simplified scheme of the experimental setup, which is a modification of the one presented in Ref. [10], is shown in Fig. 4. It consists of a halogen lamp (Halostar 64440 S from OSRAM GmbH) as the light source, a 20-mm-long $LiIO_3$ crystal cut for Type-I interaction, $\theta = 35°$, and an ANDOR iDus420-OE camera cooled down to $-55\,°C$ as a light sensor. Colored glass filters F1 and F2 provide isolation of the source light passing directly to the CCD sensor up to 10^{-15}. The filters in combination with the transmittance of the rest of the optics formed a pump bandwidth of 0.73–1.2 μm and a detection bandwidth of 390–550 nm. The pump beam is formed by two complex lenses L1 (focal length $f = 50$ mm achromat) and L2 (two lenses with $f = 420$ mm mounted side by side) with the image of the tungsten wire formed inside the nonlinear crystal. The iris aperture A1 controls the angular bandwidth of the pump, maintaining a uniform angular distribution up to 75 mrad. The angular bandwidth without the aperture is 150 mrad; some angular components are cut by the aperture of the mirror M2 and therefore the angular spectrum is not perfectly uniform. The SH radiation passing through the long-wave cutoff filter F2 is imaged from the nonlinear crystal onto the CCD camera by the lens L3 (combination of $f = 178$ mm and $f = 100$ mm achromats).

The power of the second harmonic shows a second-order dependence on pump power when the rest of the parameters of the pump (angular and frequency spectra) are kept constant; see [2,10]. Characterization of the upconverted field is rather complicated because of very low power conversion efficiency. The SH power is too low to be sent into the spectrometer in order to record the wavelength spectra directly. An insufficient amount of light may be fed through the input slit of the spectrometer because of poor coherence, which prevents the SH beam from being focused into a small spot. Therefore, the interference filters IF were used in order to evaluate SH spectra without significant modification of the existing setup. The dependence of the SH wavelength on crystal orientation may be obtained by recording the dependences with multiple interference filters. A set of Lorenz function transmittance filters with bandwidth 5–9 nm was used to measure multiple power dependences on crystal orientation. The resulting SH peak power wavelength dependence on orientation of the crystal is shown in Fig. 5. In this figure the measured curve is compared to the calculated angular dispersion law. The theoretical dispersion law was obtained from the condition $h = 0$. Good agreement between experiment and theory was obtained.

Evaluation of the spectrum profile relies on the idea that the wavelength spectrum of the pump is very broad, and

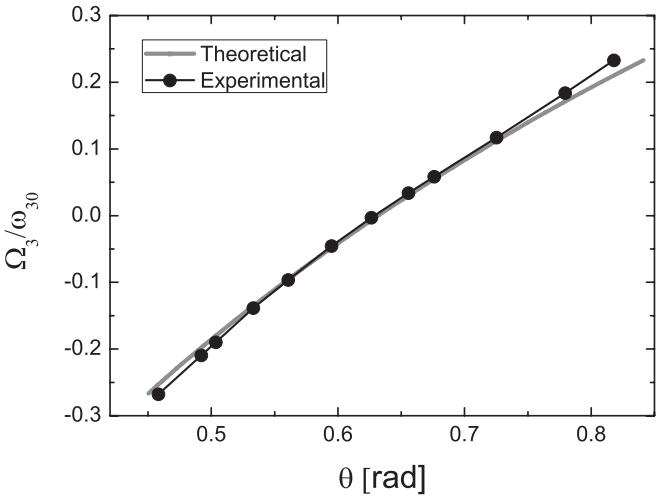

FIG. 5. Measured (black line) and calculated (gray line) angular dispersion law of the second harmonic (obtained as second-harmonic power peak). $LiIO_3$ crystal, type-I phase matching. The angle θ is calculated with respect to the optical axis of the crystal. Central wavelength of the fundamental wave $\lambda_{10} = 905$ nm.

it can be expected that the SH spectrum is dependent on rotation of the nonlinear crystal. Whatever the profile of the SH spectrum, it will change rather uniformly, mainly by shifting the central frequency. As a result, by rotation of the crystal and recording of the power passing through the narrowband filter, a signal equivalent to that of a convolution transformation is obtained. The SH spectrum shown in Fig. 6 was obtained by deconvoluting the result of a crystal rotation experiment, performed with a Gaussian transmittance filter of 7 nm bandwidth (full width at half maximum) at 455 nm. The correspondence of the SH central wavelength to a certain crystal orientation was obtained from the results in Fig. 5. The experimental data in Fig. 6 are compared to the theoretical ones. In the experiment the frequency spectral width of the fundamental wave, $a = 0.28$, is much larger than the angular spectral width, $b = 0.032$. Thus the frequency spectral width of the SH wave is determined by the parameter b rather than by a [Fig. 2 (right)]. The calculated spectral profile at $h = 0$ as well as the measured SH spectrum are depicted in Fig. 6. The reason for the difference in the spectra could be the theoretical assumption that the spectrum of the fundamental wave is Gaussian. In the experiment, the frequency as well as the angular spectral profile differ from those of a Gaussian profile. The measured as well as the calculated frequency spectral width is ∼20 nm. The experimentally measured power conversion efficiency was equal to 4.8×10^{-12}. A value of the same order was obtained in [2]. The theoretical conversion efficiency $\mu = \frac{\langle |A_3|^2 \rangle}{\langle |A_1|^2 \rangle}$ was evaluated by use of Eq. (18). An experimental value $\langle |A_1|^2 \rangle = A_{10}^2 = \frac{1}{4\pi} S_0 ab\omega_{10} k_{10}$ was obtained from the equation $A_{10}^2 = 2I/(c\varepsilon_0 n_{10})$, where $I = P/s$ is the intensity of the fundamental wave, and $P = 130$ mW and $s = 0.63$ cm^2 are the power and irradiated area, respectively. We also took into account that the input light was not linearly polarized, and that the polarization factor was equal to 0.6. As a result, the obtained efficiency μ at $\lambda_{30} = 475$ nm and crystal length $z = 2$ cm was 3.2×10^{-10}.

The SH power dependence on angular bandwidth of the pump is shown in Fig. 7. The present measurement may answer whether the pump acts as a superposition of independent pump portions or as an ensemble. The power of the pump increases by a square law, increasing the angular bandwidth of the constant radiance source. The irradiated area in the crystal also remains unchanged. The SH power dependence on angular bandwidth would be of the second order if the pump acted as a superposition of noninteracting waves, each in its own spatial acceptance bandwidth range, which could be expected, taking into account that the acceptance bandwidth, in the case of a monochromatic fundamental wave for a 2-cm-length crystal, is 0.3 mrad. The dependence, recorded experimentally and obtained by simulation, is of the fourth order, which means that the whole wave packet acts simultaneously and the SH

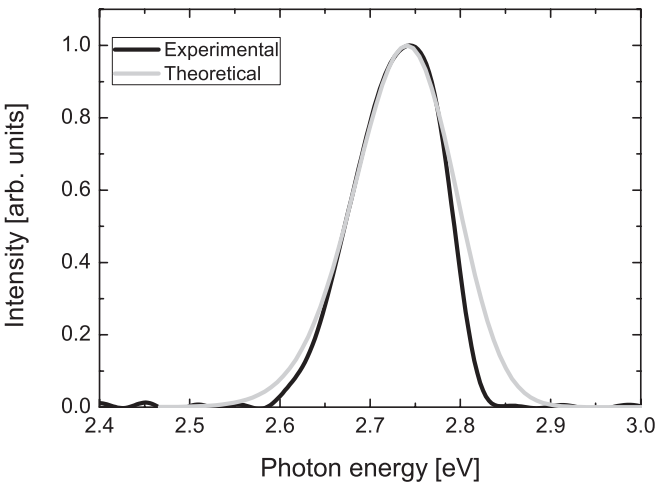

FIG. 6. Measured spectrum of the second harmonic (black line) and calculated spectral profile at $h = 0$, Eq. (13) (gray line). Crystal length $z = 2$ cm. $LiIO_3$ crystal, type-I phase matching. Central wavelength of the fundamental wave $\lambda_{10} = 905$ nm. Parameters $a = 0.28$, $b = 0.032$.

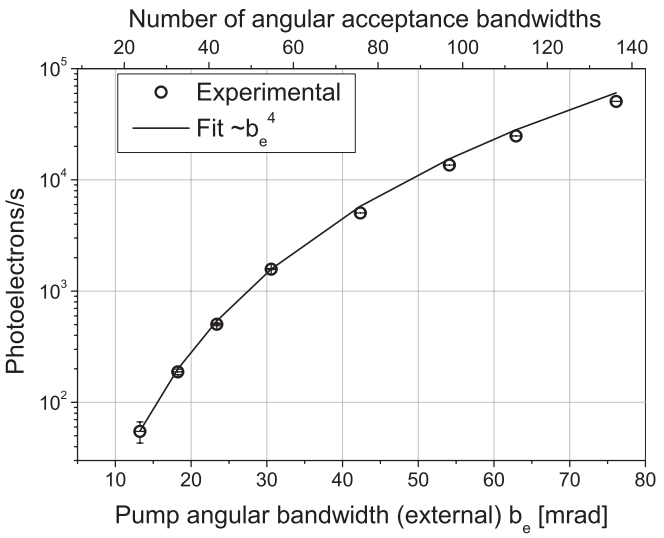

FIG. 7. Dependence of the output power of the second harmonic on external angular bandwidth b_e of the fundamental wave. Circles, measured; line, fit of the fourth order.

power still rises by a second-order dependence on pump power and does not depend on the angular content of the pump.

V. CONCLUSIONS

The theory of SH generation by an incoherent fundamental wave with simultaneous temporal and spatial walk-offs has been developed. It is revealed that SH radiation generated by incoherent light obeys a linear angular dispersion law which is determined by the temporal as well as the spatial walk-off. It is demonstrated that the power of the SH increases with pump power as a quadratic law independently of its angular content, if the relative frequency bandwidth of the fundamental wave $\Delta\Omega_1/\omega_{10}$ significantly exceeds the width of its angular spectrum $\Delta\theta_1$ ($a \gg b$). As a result, we conclude that the acceptance angle in SH generation by incoherent waves is caused by the angular bandwidth of the fundamental wave. The significant enhancement of the acceptance angle in comparison with the case of a monochromatic fundamental wave is conditioned by the angular dispersion of the SH radiation. The frequency spectrum of the SH radiation is determined by the angular bandwidth of the fundamental wave and the angular dispersion of the SH radiation. It is shown that the dependence of the SH spectral radiance on crystal length is greater than linear ($\sim z^{3/2}$). In this case an enhancement of the SH spectral radiance in comparison with that of the fundamental wave is possible. A good agreement between theoretical and experimental data was obtained.

[1] P. A. Franken, A. E. Hill, C. W. Peters, and G. Weinreich, Phys. Rev. Lett. **7**, 118 (1961).
[2] D. H. McMahon and A. R. Franklin, J. Appl. Phys. **36**, 2073 (1965).
[3] D. H. McMahon and A. R. Franklin, J. Appl. Phys. **36**, 2807 (1965).
[4] D. H. McMahon, J. Appl. Phys. **37**, 4832 (1966).
[5] A. Picozzi and M. Haelterman, Phys. Rev. Lett. **86**, 2010 (2001).
[6] A. Picozzi and M. Haelterman, Phys. Rev. E **63**, 056611 (2001).
[7] A. Piskarskas, V. Pyragaite, and A. Stabinis, Phys. Rev. A **82**, 053817 (2010).
[8] H. Wang and A. M. Weiner, IEEE J. Quantum Electron. **39**, 1600 (2003).
[9] D. N. Nikogosyan, *Properties of Optical and Laser-Related Materials. A Handbook* (Wiley, New, York, 1997).
[10] G. Tamošauskas, Opt. Commun. **284**, 5376 (2011).